Projecting MRI brain images for the detection of Alzheimer's Disease

Conference Paper *in* Studies in health technology and informatics · December 2014

DOI: 10.3233/978-1-61499-474-9-225 · Source: PubMed

6 authors, including:

Francisco Jesús Martínez-Murcia
University of Granada
60 PUBLICATIONS **275** CITATIONS

SEE PROFILE

Juan M Gorriz
University of Granada
368 PUBLICATIONS **3,600** CITATIONS

SEE PROFILE

Ignacio Alvarez Illan
University of Granada
120 PUBLICATIONS **1,642** CITATIONS

SEE PROFILE

Projecting MRI brain images for the detection of Alzheimer's Disease.

Francisco Jesús MARTÍNEZ-MURCIA [a], Juan Manuel GÓRRIZ [a,1], Javier RAMÍREZ [a], Ignacio Álvarez ILLÁN [a], Diego SALAS-GONZÁLEZ [a], Fermín SEGOVIA [b], for the Alzheimer's Disease Neuroimaging Initiative [2]

[a] *Dept. of Signal Theory, Networking and Communications. 18071 University of Granada, Spain*

[b] *Cyclotron Research Centre, University of Liège, Liège, Belgium*

Abstract. Recent advances in the process of diagnosis of neurodegenerative diseases, such as Alzheimer's Disease, rely on the use of molecular imaging that allow the interpretation of different metabolic biomarkers in the brain. However these procedures are considered of invasive nature, as they involve the injection of radioactive markers. On the other hand, Magnetic Resonance Imaging (MRI) is perhaps the most widely used and less invasive medical imaging technique, although its ability to detect Alzheimer's Disease has revealed limited. In this paper, a new method that simplifies the process of analysing 3D MRI brain images using a two dimensional projection is proposed. Our system outperforms other methods that use MRI, achieving up to a 86% of accuracy and significantly reducing the computational load. Additionally, it allows the visual analysis and interpretation of the images, which can be of great help in the diagnosis of this and other types of dementia.

Keywords. MRI, Alzheimer's disease, Computer Aided Diagnosis, Projections

1. Introduction

Alzheimer's Disease is nowadays the most common neurodegenerative disorder in the occidental world, but its early diagnosis remains a challenge. Medical imaging has become of great help in this task, as new functional imaging techniques and radiopharmaceuticals are being developed. However Magnetic Resonance Imaging (MRI), for it is safer and non-invasive, remains standard in clinical diagnosis. However, the images are usually analysed by visual inspection or using semi-quantitative methods. Therefore, more automatic methods not relying on the examiner subjectivity are desirable [10].

[1] Corresponding Author: J. M. Górriz, Dept. of Signal Theory, Networking and Communications. 18071 University of Granada, Spain; E-mail: gorriz@ugr.es.

[2] Data used in preparation of this article were obtained from the Alzheimer's Disease Neuroimaging Initiative (ADNI) database (`adni.loni.usc.edu`). As such, the investigators within the ADNI contributed to the design and implementation of ADNI and/or provided data but did not participate in analysis or writing of this report. A complete listing of ADNI investigators can be found at: `http://adni.loni.usc.edu/wp-content/uploads/how_to_apply/ADNI_Acknowledgement_List.pdf`

Numerous works have explored the capacity of MRI for detecting and predicting AD using several parameters, as the cortical thickness [2], analysis of Regions of Interest (ROIs) [7] or compared measures of brain region atrophy [6]. Nevertheless they often rely on either a-priori anatomical knowledge or complex underlying algorithms. In most cases are based on the segmentation of brain MRI images, separating white matter (WM) from grey matter (GM) and using either or both of them to extract relevant parameters. As the neurodegeneration occurs mostly in the GM, procedures usually focus on this type of tissue, and obviate the WM.

In the present work we have proceeded likewise, first segmenting the available MRI images into GM and WM and then projecting these GM images onto two-dimensional maps. This latter procedure introduces the main novelty of this paper, providing visually, easily-assessable images with a significant reduction of the data size (from more than two million voxels in each MRI image to around 260,000 pixels). Later some discrimination ability measures, such as the two-sample t-Test, can be estimated, thus allowing the selection of the most discriminant pixels. This feature selection technique has been previously applied to brain images with successful results [10,9,5]. Finally, the feature vectors are classified using a linear support vector machine classifier. These supervised learning models are the state-of-the art in many recent works [5,8,10], since they are trained to maximize the margin of the separation hyperplane, leading to good generalization ability.

This paper is organized as follows. First, in Section 2, the image database used is presented, and the techniques of projection, feature selection and classification are introduced. Later, in Section 3, the results are presented and discussed, compared to the use of the raw images as an input to the classifier. Finally in Section 4 some conclusions are drawn, and future work is proposed.

2. Material and Methods

2.1. MRI Brain Image database

Data used in the preparation of this article were obtained from the Alzheimer's Disease Neuroimaging Initiative (ADNI) database (adni.loni.usc.edu). The ADNI was launched in 2003 by the National Institute on Aging (NIA), the National Institute of Biomedical Imaging and Bioengineering (NIBIB), the Food and Drug Administration (FDA), private pharmaceutical companies and non-profit organizations, as a $60 million, 5-year public-private partnership. The primary goal of ADNI has been to test whether serial magnetic resonance imaging (MRI), positron emission tomography (PET), other biological markers, and clinical and neuropsychological assessment can be combined to measure the progression of mild cognitive impairment (MCI) and early Alzheimer's disease (AD). Determination of sensitive and specific markers of very early AD progression is intended to aid researchers and clinicians to develop new treatments and monitor their effectiveness, as well as lessen the time and cost of clinical trials.

The Principal Investigator of this initiative is Michael W. Weiner, MD, VA Medical Center and University of California-San Francisco. ADNI is the result of efforts of many co-investigators from a broad range of academic institutions and private corporations, and subjects have been recruited from over 50 sites across the U.S. and Canada. The initial goal of ADNI was to recruit 800 subjects but ADNI has been followed by ADNI-

GO and ADNI-2. To date these three protocols have recruited over 1500 adults, ages 55 to 90, to participate in the research, consisting of cognitively normal older individuals (NOR), people with early or late MCI, and people with early AD. The follow up duration of each group is specified in the protocols for ADNI-1, ADNI-2 and ADNI-GO.

The database that has been used in this work is extracted from the ADNI1:Screening 1.5T (subjects who have a screening data) and contains 1075 T1-weighted MRI images, comprising 229 NOR, 401 MCI (312 stable MCI and 86 progressive MCI) and 188 AD images. This database contains MRI data from 818 subjects and repeated scans in some cases. When multiple scans of the same subject were available, the first one was selected. To prevent this study from being prevalence-dependent, 180 individuals have been randomly selected from each of the classes AD and normal controls. The same set of patients has been used in the rest of the article. The source images from the ADNI database are spatially normalized and segmented using the SPM software [1], after a skull removing procedure. Hereafter, we will use independently the segmented 360-subject Gray Matter (GM) database.

2.2. 2D Projection

The algorithm proposed to perform the 2D mapping is based on the use of spherical coordinates in the brain. A central point is set in the central voxel of the MRI image. Starting at this point, the different inclination (θ) and azimuth (φ) angles are varied, and a vector $\mathbf{r}$ that contains all the data is computed for each pair of coordinates (θ, φ) in all directions ($-180^\circ < \theta < 180^\circ$ and $-90^\circ < \varphi < 90^\circ$) at a resolution Res (default $Res = 0.5^\circ$). For each pair of coordinates, a value R is computed and it is mapped into a pixel value using $\mathbf{r}$ in different approaches:

1. A basic **brain surface** approach, which might allow our system to observe structural degeneration and tissue loss. However, this approach is focused on the outer voxel itself, so all the complex inner GM foldings are lost, which could limit the discrimination ability of the whole system.
   The value R is calculated as the distance in voxels between the central voxel and the latest value in $\mathbf{r}$ that has an intensity greater than a threshold I_{Th}, which corresponds to the outer voxel inside the brain. In this work, the value of I_{Th} is always set to 0, although it could be increased in the case of noisier images, where the outer voxel could be mistaken.
2. An **average** approach, in which the value R is computed as the average of all the values in the vector $\mathbf{r}$ at a fixed θ and φ. The resulting maps show a bigger complexity, as all the tissues and foldings crossed by $\mathbf{r}$ are projected to one single point. Nevertheless this approach maps all outer and inner features, leading to a far more representative map of the GM structure.

An example of the resulting projections for both AD and NOR patients is shown in Figure 2. We can observe some differences in the brain surface between AD and NOR patients (Figures 2(a) and 2(c) respectively), although its detail level might be less relevant than the one found using the average projection. In this latter approach (Figures 2(b) and 2(d)) some underlying structure of the sulcal pattern can be inferred. Furthermore, a greater difference between AD and NOR subjects can be established by means of a greater complexity and thickness of the sulci projections.

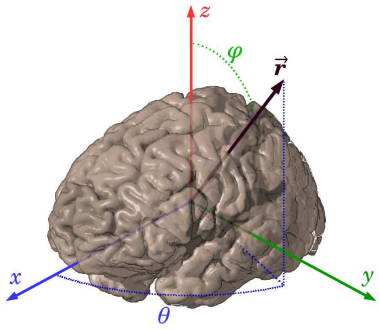

Figure 1. Illustration of the computation of the vector **r** at each coordinate (θ, φ).

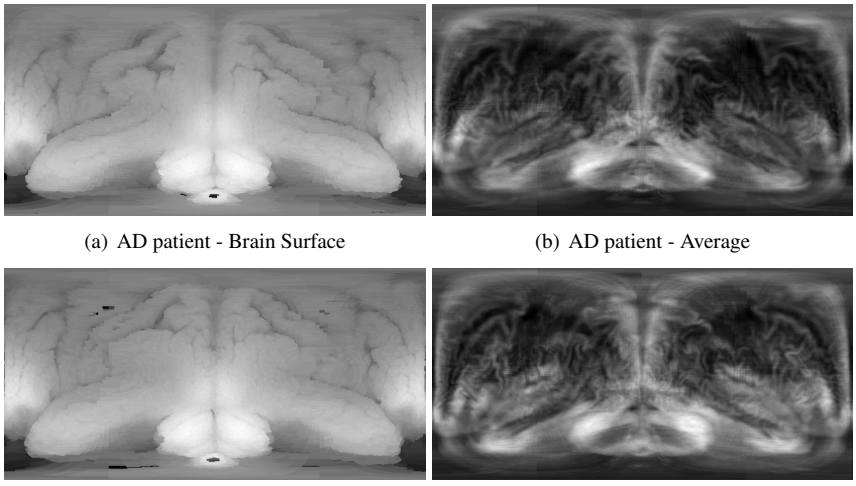

(a) AD patient - Brain Surface

(b) AD patient - Average

(c) NOR patient - Brain Surface

(d) NOR patient - Average

Figure 2. Resulting projection of the same AD and NOR subject (Gray Matter) for: (a) and (c) Surface Approach and (b) and (d) Average Approach.

2.3. Feature selection

Once we have projected the 3D MRI images onto two-dimensional, 720×360-pixel maps, we can use the entire projection as the feature vector. However, some improvements can be made to this strategy, by selecting the most useful pixels using their discrimination ability. To compute this, we will use the t-value obtained using the well-known two-sample t-Test with independent variance estimation as in [4] to rank the texture features and further reducing the dimensionality of the feature vector.

Our method extracts a discrimination vector ($\mathbf{s}$), that contains one discrimination value per pixel in the projection $\mathbf{x}_0$. Note that each projection $\mathbf{x}_0$ must be previously labelled with its corresponding class (Ω_1 and Ω_2, NOR and AD respectively), as it corresponds to a different image. Then, we obtain a vector $\mathbf{x}_{rank}$ by sorting $\mathbf{x}_0$ in descending order of discrimination ability, using the values in $\mathbf{s}$. Finally, first n features (where n depends on the total number of pixels N and the ratio of selected pixels, ranging from

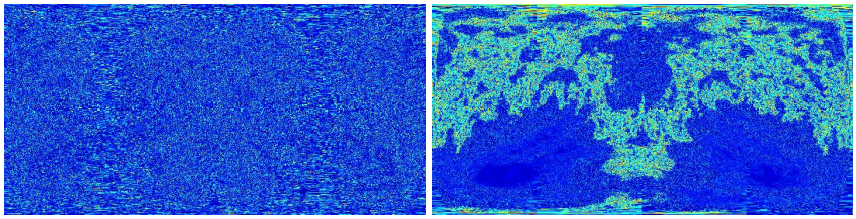

(a) Surface - t-values (b) Average - t-values

Figure 3. t-values for (a) Surface and (b) Average projections.

0.05 to 1) are selected from $\mathbf{x}_{rank}$ as follows:

$$\mathbf{x} = \mathbf{x}_{rank}(1:n) \tag{1}$$

For each pixel, the two-sample t-Test is computed as follows:

$$t = \frac{\bar{\Omega}_1 - \bar{\Omega}_2}{\sqrt{\frac{\sigma^2_{\Omega_1}}{n_1} + \frac{\sigma^2_{\Omega_2}}{n_2}}} \tag{2}$$

where $\bar{\Omega}_c$ is the mean of each class, $\sigma^2_{\Omega_c}$ is the variance of each class and n_c is the number of samples in each class. We use all i -class numbers- where $\Omega_c(i) > 0$. The t-values calculated in each pixel and each projection are depicted in Figure 3.

2.4. Classification: Support Vector Machines

Support Vector Machines [11] are state-of-the-art classifiers, widely used and applied to lots of different problems, specially in pattern recognition. Being a maximum-margin classifier, and having excellent generalization ability in the linear case, they have been successfully used in a number of CAD systems [10,4,8]. The SVM problem can be defined as follows. Consider (x_i, y_i), $i = 1, \ldots N$ where $x \in R^P$ and $y_i \in -1, 1$, we have to find the maximum margin hyperplane, by solving the optimization problem that minimizes:

$$\frac{1}{2\|\mathbf{w}\|^2} \tag{3}$$

subject to

$$y_i(\mathbf{w}^T\mathbf{x}_i - b) \leq 1 \tag{4}$$

This problem can be solved using standard quadratic programming techniques and programs. In our case, where the 'gold standard' is set by visual inspection or even by cognitive tests, we can add a constraint that depends on the distance to the hyperplane, penalizing the class in non-separable classes or mislabelled samples:

$$\frac{1}{2\|\mathbf{w}\|^2} + C\sum_{i=1}^{N}\xi \tag{5}$$

subject to the constraint:

$$y_i(\mathbf{w}^T\mathbf{x}_i - b) \geq 1 - \xi_i, \mathtt{and} \xi_\mathtt{i} > 0 \tag{6}$$

3. Results and Discussion

All performance results shown here have been obtained using a 10-Fold cross-validation, as suggested in [3], reducing the variance of other widely known forms of cross-validation like leave-one-out. Accuracy, sensitivity and specificity have been computed, as we have controlled the prevalence of the samples by selecting the same number of samples in both classes.

First, we must introduce whether the projection of a MRI image onto two dimensions is worthwhile. Assuming that a computational load reduction has resulted of projecting the images, as the amount of data falls significantly in more than one order of magnitude, we should focus on the performance of these images and the information that they contain. Therefore, we will compare the discrimination ability of using either raw MRI images as in the Voxels as Features (VAF) paradigm or the projected images, which is considered a good indicator of the visual analysis performed by experts [10].

For this purpose, we will use the entire vectorised MRI image, then selecting the most discriminant voxels using the algorithm defined previously in Section 2.3. After applying this feature selection we obtain the performance shown in Figure 4. We obtain performance values in the range of 0.78 to 0.83 of accuracy. Note that the last value corresponding to 100% of the selected voxels is exactly as if no feature selection was applied, corresponding to the widely-known VAF approach.

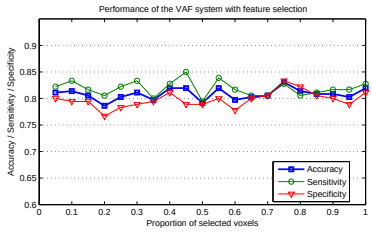

Figure 4. Performance of the VAF approach with our feature selection algorithm.

Regarding the projections it is useful to analyse them (Fig. 2) and their statistical significance masks (Fig. 3), before looking at the cross-validation results. As we can see in Fig 2, surface and average projection show very different characteristics, and just by looking at these, we can infer that the most considerable amount of information is contained in the average projection. This projection offers more relevant features for the characterization of brain atrophy, as we can observe that the lines that represent the sulci are significantly thinner, and their density is smaller in AD patients. Conversely, this feature is not easily interpreted when analysing the raw MRI images, which represents an interesting improvement. It is also interesting that the surface projection itself lacks several details of the brain, since most of the cortex folding fold on itself, and we can only extract the outer relief and not the underlying foldings.

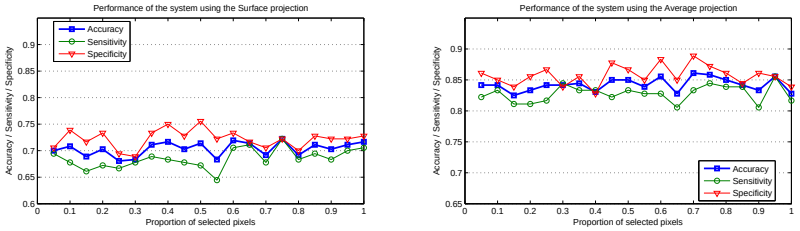

(a) Surface projection (b) Average projection

Figure 5. Variation in the performance values obtained with the automatic selection of features when using the (a) Surface images and (b) average projections.

Now analysing Figure 3, we can see that the t-Test is far more efficient in selecting pixels from the average projection than in the surface projection. It is highly visible that the areas where the sulci are more visible have better discrimination ability than others in this type or projection, and therefore more information can be extracted from these. On the contrary, in the surface approach, the distribution of the t-values resembles a noise distribution, probably due to both anatomical differences between subjects and a smaller amount of information, given that it selects only the last voxel in the vector $\mathbf{r}$.

Consequently, the analysis of the performance of the classifier leads to the same conclusion. As we can observe in Figure 5, the average projection achieves higher accuracy, sensitivity and specificity results than the surface projection in almost every case. Furthermore, the surface projection obtains worse results than the VAF approach, which is another proof of its lack of relevant information. It is interesting to note that, in both cases, the performance values remain similar while changing the proportion of selected pixels, which is a good indicator of the suitability of our feature selection algorithm. Furthermore, good performance values around 85% of accuracy are obtained despite the number of pixels selected. As a result, it allows us to further reduce the dimension of the feature vector from 260281 pixels in the projections to even a 5% of this amount, 13014 pixels, which improves the computational efficience.

To summarize, in Table 1 we show the exact performance results with confidence bounds of our system at the optimum operation point. As we have previously commented, the best performance is achieved by the projection that contains the higher amount of information: the average projection. It outperforms the MRI VAF approach, and similarly it does with the surface projection, revealing its ability and robustness in detecting AD patterns from MRI images.

System	**Accuracy**	**Sensitivity**	**Specificity**
MRI-VAF	0.831 ± 0.039	0.828 ± 0.038	0.833 ± 0.038
Surface Projection	0.722 ± 0.046	0.722 ± 0.046	0.722 ± 0.046
Average Projection	0.861 ± 0.035	0.833 ± 0.038	0.889 ± 0.033

Table 1. Comparison of our proposed system, using both types of projections, with the baseline MRI-VAF at the operation point.

4. Conclusions

In this paper, a new technique for projecting the Magnetic Resonance Images (MRI) onto a two-dimensional map has been proposed. Two different approaches have been tested, the first one projecting the surface of the brain and the second one an average of all voxels in one radial vector. Later, a feature selection algorithm based on two-sample t-Test has been used to select the most discriminant pixels, and the whole system has been tested.

Our system proves to be robust against changes in the amount of selected voxels, and it demonstrates its ability in the detection of Alzheimer's Disease using MRI images, achieving up to a 86% of accuracy. Furthermore, it reduces significantly the computational load, as can utterly obtain this performance using only 13014 features out of the 2122945 voxels that the MRI images contain, a total reduction of two magnitude orders.

The analysis of the projections itself reveals promising, since they can be visually analysed and interpreted, for example, by examining the sulcal projections in the average approach. In this type of projection, the thinner and less dense lines are a good indicator of brain atrophy, a good predictor of Alzheimer's Disease. These projections also allow further processing that could be developed in the future. Particularly, the addition of texture characterization methods, cartographic algorithms and modifications to the projections proposed in this paper could pave the way for improving the performance of the present system and implementing new techniques suitable for other diseases.

Acknowledgements

This work was partly supported by the MICINN under the TEC2008-02113 and TEC2012-34306 projects and the Consejería de Innovación, Ciencia y Empresa (Junta de Andalucía, Spain) under the Excellence Projects P09-TIC-4530 and P11-TIC-7103.

Data collection and sharing for this project was funded by the Alzheimer's Disease Neuroimaging Initiative (ADNI) (National Institutes of Health Grant U01 AG024904) and DOD ADNI (Department of Defense award number W81XWH-12-2-0012). ADNI is funded by the National Institute on Aging, the National Institute of Biomedical Imaging and Bioengineering, and through generous contributions. ADNI data are disseminated by the Laboratory for Neuro Imaging at the University of Southern California.

References

[1] K.J. Friston, J. Ashburner, S.J. Kiebel, T.E. Nichols, and W.D. Penny. *Statistical Parametric Mapping: The Analysis of Functional Brain Images*. Academic Press, 2007.

[2] Xiao Han, Jorge Jovicich, David Salat, Andre van der Kouwe, Brian Quinn, Silvester Czanner, Evelina Busa, Jenni Pacheco, Marilyn Albert, Ronald Killiany, et al. Reliability of mri-derived measurements of human cerebral cortical thickness: the effects of field strength, scanner upgrade and manufacturer. *Neuroimage*, 32(1):180–194, 2006.

[3] R Kohavi. A study of cross-validation and bootstrap for accuracy estimation and model selection. In *Proceedings of International Joint Conference on AI*, pages 1137–1145, 1995.

[4] FJ Martinez-Murcia, JM Górriz, J Ramírez, M Moreno-Caballero, M Gómez-Río, Parkinson's Progression Markers Initiative, et al. Parametrization of textural patterns in 123i-ioflupane imaging for the automatic detection of parkinsonism. *Medical physics*, 41(1):012502, 2013.

[5] Francisco Jesús Martínez-Murcia, JM Górriz, Javier Ramírez, Carlos García Puntonet, and IA Illán. Functional activity maps based on significance measures and independent component analysis. *Computer methods and programs in biomedicine*, 111(1):255–268, 2013.

[6] Linda K McEvoy and James B Brewer. Quantitative structural mri for early detection of alzheimer's disease. *Expert Rev Neurother*, 10(11):16751688, Nov 2010.

[7] Andrés Ortiz, Juan M Górriz, Javier Ramírez, Francisco J Martinez-Murcia, Alzheimer's Disease Neuroimaging Initiative, et al. Automatic roi selection in structural brain mri using som 3d projection. *PLOS ONE*, 9(4):e93851, 2014.

[8] A. Rojas, J.M. Górriz, J. Ramírez, I.A. Illán, F.J. Martínez-Murcia, A. Ortiz, M. Gómez Río, and M. Moreno-Caballero. Application of Empirical Mode Decomposition (EMD) on DaTSCAN SPECT images to explore Parkinson Disease. *Expert Systems with Applications*, 40(7):2756 – 2766, 2013.

[9] D. Salas-Gonzalez, J. M. Górriz, J. Ramírez, I. A. Illán, M. López, F. Segovia, R. Chaves, P. Padilla, and C. G. Puntonet. Feature selection using factor analysis for Alzheimer's diagnosis using F-FDG PET images. *Medical Physics*, 37(11):6084–95, Nov 2010.

[10] J. Stoeckel, N. Ayache, G. Malandain, P. M. Koulibaly, K. P. Ebmeier, and J. Darcourt. Automatic Classification of SPECT Images of Alzheimer's Disease Patients and Control Subjects. In *Medical Image Computing and Computer-Assisted Intervention - MICCAI*, volume 3217 of *Lecture Notes in Computer Science*, pages 654–662. Springer, 2004.

[11] V. Vapnik. *Statistical learning theory*. John Wiley and Sons, New York, 1998.